biij

Improvement in diagnosis of breast tumour using ultrasound elastography and echography: A phantom based analysis

K Kumar [*,1], M.Tech, ME Andrews[2], PhD, V Jayashankar[1], PhD, AK Mishra[2], PhD, S Suresh[3], MBBS

1 Department of Electrical Engineering, IIT Madras, Chennai, India
2 Department of Chemistry, IIT Madras, Chennai, India
3 Mediscan Systems, Chennai, India

ABSTRACT

Due to the isoechoic nature of lesions and their poor contrast with neighbouring tissue, a lesion may remain undetected in ultrasound B mode imaging for cancerous tissue. Imaging of the elastic properties of tissue provides new information which is collateral to tissue pathology. This study provides quantitative analysis of improvements in tumour diagnosis when the ultrasound B mode imaging is combined with elastography. Quantification was based on the textural parameters measured from the ultrasound B mode image and strain measured from the elastogram. The ability of a parameter to discriminate between diseased cases and normal cases was evaluated using receiver operating characteristic (ROC) analysis. Polyacrylamide gel based tissue mimicking phantoms with embedded inclusions of varying stiffness were used for the analysis. © 2009 Biomedical Imaging and Intervention Journal. All rights reserved.

Keywords: Elastography; classifier; ROC; texture; tissue phantom

INTRODUCTION

Particularly when the task at hand is to differentiate between malignant tumours and other possibly benign conditions, non-invasive identification of a breast tumour is a challenging area of medical diagnosis. Prior to the advent of diagnostic imaging, the oldest method of detection involved palpation. While palpation is understandably simple, it is nevertheless just a qualitative assessment and can only be applied to superficial organs. Malignant tumours feel harder than benign ones and this physical property is related to their coefficient of elasticity. The elasticity of soft tissues depends on their molecular building blocks (fat, collagen, etc.) and on their microscopic and macroscopic structural organisation of these blocks [1-3]. Pathological changes are generally correlated with changes in tissue stiffness as well. In many cases, the lesion may not possess sufficient echo graphic properties and therefore it avoids detection using normal B mode ultrasound. As the echogenecity and the stiffness of tissue are generally uncorrelated, it is expected that imaging tissue stiffness will provide new information that is related to tissue structure and or pathology [3].

* Corresponding author. Present address: c/o Prof. Jayashankar V, ESB 317A, Measurements and Instrumentation Lab, Department of Electrical Engineering, IIT Madras, Chennai – 600036, India.
Tel: +91-44 -2257 5404; Fax: +91-44-2257 0509;
E-mail: kishorekumar.cki@gmail.com (Kishore Kumar).

K Kumar et al. Biomed Imaging Interv J 2009; 5(4):e30

2
This page number is not
for citation purposes

Elastography is a method of estimating the elastic properties of biological tissues [3-7]. Elastograms are obtained by comparing ultrasound echo data obtained before and after a slight compression of the tissue. The results of the comparison are displayed as an image, where soft areas appear white and hard areas appear black. Garra et al. [8] used ultrasound elastography for the examination of breast lesions using a 5 MHz linear array transducer. The elastogram and corresponding sonogram were evaluated by a single observer for lesion visualisation, relative brightness and margin definition. The mean depth and width of the lesion on the elastogram and sonogram were measured and used as parameter for differentiating benign and malignant lesions. Andrej et al. [9] and Rago et al. [10] performed real time elastography on the thyroid lesions. All elastograms were evaluated for the lesion visibility, relative brightness, and margin regularity and definition by using a four point scale. Zhi et al. [11] evaluated the capability of ultrasound elastography in differentiating between benign and malignant lesions of the breast, and compared this with conventional sonography and mammography. They concluded that ultrasound elastography is superior to conventional sonography, and furthermore is superior or equal to mammography in differentiating between benign and malignant lesions in the breast. By combining ultrasound elastography and sonography, accuracy of detection can be improved greatly, while retaining the potential to reduce unnecessary biopsy.

None of the above studies attempted a quantitative analysis of the improvement in classification accuracy when ultrasound elastography is combined with echography. The main focus of this study is to quantify the improvement in diagnosis of tumours by combining the ultrasound B mode imaging with elastography. Quantification is based on the textural parameters measured from the ultrasound B mode image and strain measured from the elastogram.

MATERIALS AND METHODS

Phantom preparation

Polyacrylamide gel based tissue mimicking phantoms [12] were designed for study and analysis. The polymerisation of acrylamide was carried out in deionised water at room temperature using bisacrylamide as the cross linker, and mmonium persulfate (APS) and tetramethylethylenediamine (TEMED) as a pair of redox initiators. Fine particles of titanium dioxide were used to control the echogenecity of the gel. The elasticity of the phantom was varied by adjusting the acrylamide concentration so that it covered a wide range of normal to pathological tissue stiffness.

Acoustic properties of the phantoms were measured using the pulse-echo-transmit-receive principle, with a single element transducer of 5 MHz centre frequency. Young's modulus of the sample was measured using the unconfined compression test. A variable compression
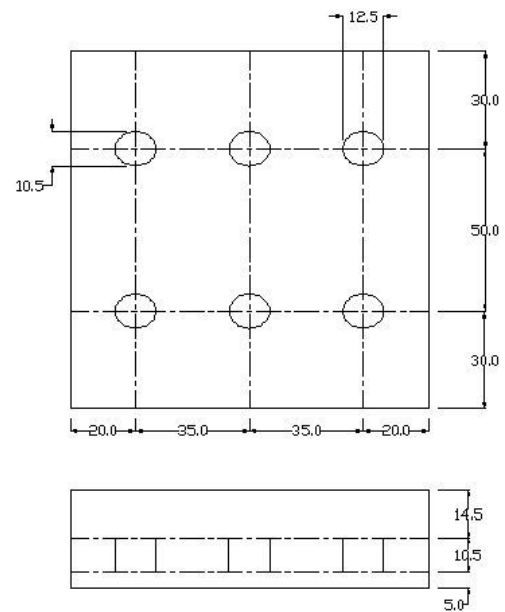

Figure 1 Plan and elevation of a typical phantom with six embedded inclusions of varying stiffness. (Phantom details: prepared with 8% acrylamide, 0.06% initiator and 40% TiO$_2$ Concentration of acrylamide in inclusions was varied from 6% to 20%. Concentration of TiO2 and initiator was same in all the inclusions and is equal to 40% and 0.06% respectively). All measurements are in mm.

Figure 2 External view of the phantom.

load was applied on the sample and corresponding deformation is measured. From these data, stress-strain characteristics of the sample were plotted and the modulus was measured.

Two categories of phantoms were designed with embedded inclusions of varying stiffness. In the first category the elasticity was maintained constant and echogenecity was varied, thus producing isoechoic (indistinguishable from surrounding tissue), hyperechoic

K Kumar et al. Biomed Imaging Interv J 2009; 5(4):e30

3
This page number is not
for citation purposes

(appearing brighter than surrounding tissue), hypoechoic (appearing darker than surrounding tissue) and anechoic lesions (those without echoes). In the second category echogenecity was kept constant and elasticity was varied.

The plan and elevation of a typical phantom from the second category is shown in Figure 1. The external view of the phantom is shown in Figure 2. The ultrasound B mode and elastographic behaviour of these lesions was analysed using image processing methods.

Image acquisition

Ultrasound B mode and elastograms were acquired using Siemens ACUSON Antares [13], at Mediscan System, Chennai. Linear array transducer VF 7-3 with a probe frequency of 5 MHz was used. Initially, B mode image of the region of interest (ROI) was obtained and then a slight compression was applied by pressing the transducer on the surface. Built- in software present in the system generated the elastogram by comparing the pre-compressed and post-compressed RF signals, and displayed these adjacent to the B mode image for comparison and more accurate diagnosis.

Tissue characterising parameters

Texture parameters were measured to quantify the B mode images [14-15]. The first order parameters used in this study were mean value, variance, skewness, kurtosis, energy and entropy, and accounted for variations in intensity without spatial reference. These parameters were measured by computing the image histogram, the shape of which provided many clues as to the character of the image. Second order texture parameters were extracted from the normalised co-occurrence matrices [16] and include angular second momentum, correlation, inertia, absolute value, inverse difference, entropy and maximum probability. While first order texture parameters cannot completely characterise texture, second order texture parameters account for changes in the spatial arrangements of intensities.

Quantitative analysis of parameters

The ability of a test to discriminate between diseased cases and normal cases was based on receiver operating characteristic (ROC) analysis. The ROC curve represents a plot describing the classifier's true positive (TP) detection rate against its false positive (FP) rate [17-18]. In medical imaging the TP rate is commonly referred to as sensitivity and (1.0 – FP rate) is referred to as specificity.

The histograms of each parameter were calculated to obtain the distribution of parameter values for both normal and tumour groups. Specificity (S_p) and sensitivity (S_e), were determined as:

$$S_e = \frac{TP}{FN + TP} \qquad S_p = \frac{TN}{TN + FP} \qquad (1)$$

where *TN* is true negative and *FN* is false negative.

By changing the threshold, TP and FP rate can be varied. Plotting sensitivity against specificity, for different threshold values, ROC curve can be obtained. The area under the ROC curve (A_{ROC}) is an accepted method of comparing classifier performance, and a perfect classifier ought to have a TP rate of 1.0 and a FP rate of 0.0, resulting in A_{ROC} of 1.0. Values of $0.5 < A_{ROC} \leq 1$ indicate the potential of the respective parameters to differentiate between the existence and absence of tumours.

Bayesian classifier

The probability that a sample belongs to class C_i, given that it has a feature value x denoted by P(C_i/x) can be computed as [19]:

$$g_i(x) = P(C_i / x) = \frac{p(x / C_i)P(C_i)}{\sum_{j=1}^{C} p(x / C_j)P(C_j)} \qquad (2)$$

where p(x/C_i) is the conditional probability of obtaining feature value x given that sample is from class C_i, P(C_i) is the prior probability that a random sample is a member of class C_i and C is the total number of classes. For a two dimensional case, the normal density function can be written as:

$$p(x) = \frac{1}{2\pi|C_v|} e^{\left[-\frac{1}{2}(x-\mu)^t C_v^{-1}(x-\mu)\right]} \qquad (3)$$

where C_v is the covariance matrix, μ is the mean vector, $|C_v|$ and C_v^{-1} are the determinant and inverse of covariance matrix respectively.

A Bayesian classifier can be trained by determining the mean vector, and the covariance matrices for the normal and tumour classes from the training data. For the training corresponding to Class 1 (tumour) and Class 2 (normal) data, mean vector and covariance matrix were calculated separately. The parameters with highest values of A_{ROC} were chosen as the best performing parameters. Using these parameters, a discriminant function for a two class case can be defined as:

$$g(x) = g_1(x) - g_2(x) \qquad (4)$$

where $g_1(x)$ and $g_2(x)$ are discriminant functions corresponding to two classes. We use the following decision rule: decide class 1 if g(x) > 0; otherwise decide class 2. [19]

RESULTS

The acoustic properties of the phantoms used for the analysis are shown in the Table 1 along with corresponding parameters for human tissue [20-21]. Figures 3, 4 and 5 show the ultrasound B mode and elastogram of the different lesions analysed.

They are hyperechoic (Figure 3), anechoic (Figure 4b) and isoechoic (Figure 5) lesions respectively. In the elastogram , soft areas are represented by white and hard areas are represented by black. Figure 6 shows

K Kumar et al. Biomed Imaging Interv J 2009; 5(4):e30

4
This page number is not
for citation purposes

the areas on the B mode image and the elastogram for the measurement of parameters.

From the designed phantoms, a total of 28 images from the embedded inclusions were obtained. Separation of normal regions and tumour regions was based on the Young's modulus of the inclusion, which in turn was controlled by the concentration of monomers. An inclusion with a Young's modulus of greater than 60 kPa was considered as a stiffer region and therefore deemed to be a tumour. Based on this criterion, among 28 inclusions, 7 were selected as normal, and the remaining 21 as tumour regions.

ROC analysis was performed for all 14 parameters, and finally parameters with $A_{ROC} > 0.5$ were used as input to the classifier. From the group of first order texture parameters, mean (M), skewness (SK) and entropy (ENT) were used. The parameters used from the second order texture parameters were angular second momentum (ASM) and maximum probability (max_prob). In addition, average strain (STR) estimated from the elastogram was also included.

Results of the parameter evaluation using A_{ROC} are shown in Table 2. The total number of cases used for training was 5 normal and 8 tumours. Classification results with and without the average strain parameter (STR) are shown in the Table 3.

DISCUSSION

The acoustic parameters of the phantoms designed in this study closely matched those of human tissue (Table 1). The lesions were clearly distinguishable in the elastogram, even though they appear almost similar in B mode. These results are clearly evident from the images shown in Figures 3, 4 and 5. In this study, along with average strain estimated from the elastogram, several tissue characterising parameters were used, all estimated from ultrasound B mode images. The ability of each parameter in differentiating between normal regions and tumour regions has been analysed. Class 1 included lesions whose Young's modulus is greater than 60 kPa; Class 2 included softer regions.

ROC analysis confirmed that the use of a single parameter is not recommended. And it has been shown that using high performance parameters collectively in the classification will produce an accuracy of 86.7%.

CONCLUSION

Echogenicity and elasticity of the phantoms are suitably controlled to obtain normal and pathological lesions in the phantoms. An increase in the classification accuracy was achieved following the inclusion of the average strain parameter as an additional input to the classifier. Elastography may thus be considered as one of the available diagnosis tool for improving the accuracy of the diagnosis of breast and thyroid tumours.
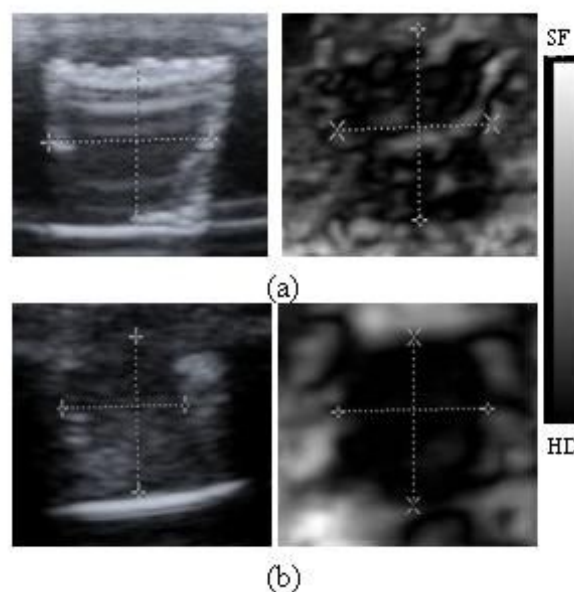

Figure 3 Ultrasound B mode image and elastogram of two solid lesions. Both the lesions appear hyperechoic in B mode but their characteristics are different in elastogram. (a) is less stiffer than (b). In elastogram black region represents hard (HD) and white region represents soft (SF). Line markings shows the width and depth of the lesion.
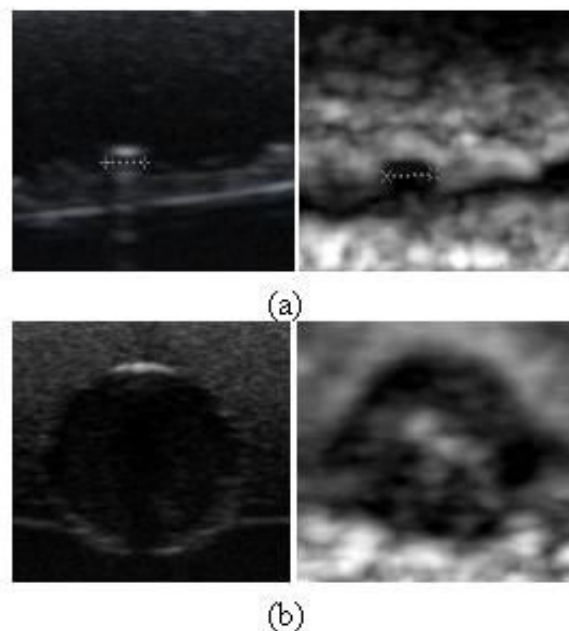

Figure 4 Ultrasound B mode image and elastogram of two lesions. (a) Very small hyperechoic lesion in B mode and hard lesion in elastogram. (b) Anechoic lesion in B mode and a Bull's eye appearance in elastogram, a typical elastographic appearance of cystic lesion.
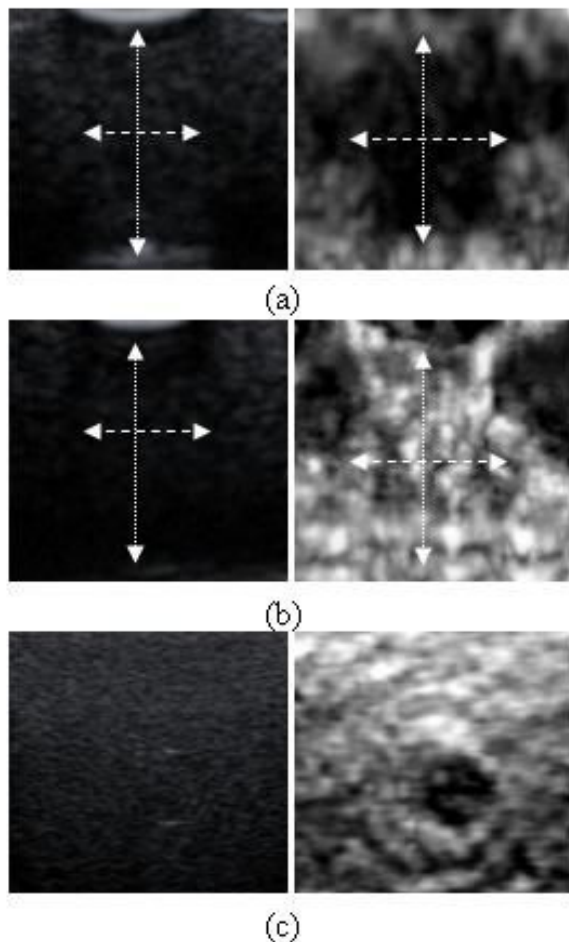
K Kumar et al. Biomed Imaging Interv J 2009; 5(4):e30

5
This page number is not
for citation purposes

Figure 5 Ultrasound B mode image and elastogram of three solid lesions. Lesions appear isoechoic in B mode but their characteristics are different in elastogram. (a) and (c) are stiffer and (b) is soft. Arrow markings show the width and depth of the lesion.

REFERENCES

1. Fung YC. Biomechanics: mechanical Properties of Living Tissues. 2nd edition. Springer, 1993.
2. Yamada H. Strength of Biological Materials. Baltimore: The Williams and Wilkins Company, 1970.
3. Ophir J, Cespedes I. Elastography: ultrasonic imaging of tissue strain and elastic modulus in vivo. European J Med Ultrasound 1996; 3:49-70.
4. Hall TJ. AAPM/RSNA physics tutorial for residents: topics in US: beyond the basics: elasticity imaging with US. Radiographics 2003; 23(6):1657-71.
5. Ophir J, Cespedes I, Ponnekanti H *et al*. Elastography: a quantitative method for imaging the elasticity of biological tissues. Ultrason Imaging 1991; 13(2):111-34.
6. Ophir J, Alam SK, Garra B *et al*. Elastography: ultrasonic estimation and imaging of the elastic properties of tissues. Proc Inst Mech Eng H 1999; 213(3):203-33.
7. Szabo TL. Diagnostic ultrasound Imaging Inside out. Elsevier Academic Press, 2004.
8. Garra BS, Cespedes EI, Ophir J *et al*. Elastography of breast lesions: initial clinical results. Radiology 1997; 202(1):79-86.
9. Lyshchik A, Higashi T, Asato R *et al*. Thyroid gland tumor diagnosis at US elastography. Radiology 2005; 237(1):202-11.
10. Rago T, Santini F, Scutari M *et al*. Elastography: new developments in ultrasound for predicting malignancy in thyroid nodules. J Clin Endocrinol Metab 2007; 92(8):2917-22.
11. Zhi H, Ou B, Luo BM *et al*. Comparison of ultrasound elastography, mammography, and sonography in the diagnosis of solid breast lesions. J Ultrasound Med 2007; 26(6):807-15.
12. Kumar K, Jayashankar V. Image processing based characterization of tissue phantoms for ultrasound elastography applications. Proc Int Conf Comp Comm Control and Instru. 2007: 395-9.
13. Siemen's Medical [Online]. Available at http://www.medical.siemens.com.
14. Wu CM, Chen YC, Hsieh KS. Texture features for classification of ultrasonic liver images. IEEE Trans Med Imaging 1992; 11(2):141-52.
15. Garra BS, Krasner BH, Horii SC *et al*. Improving the distinction between benign and malignant breast lesions: the value of sonographic texture analysis. Ultrason Imaging 1993; 15(4):267-85.
16. Materka A, Strzelecki M. Texture analysis methods - a review. Brussels: Technical university of Lodz, Institute of electronics, 1998; COST B11 report.
17. Meyer-Base A. Pattern recognition for medical imaging. Elsevier Academic Press, 2004.
18. Joo S, Yang YS, Moon WK *et al*. Computer-aided diagnosis of solid breast nodules: use of an artificial neural network based on multiple sonographic features. IEEE Trans Med Imaging 2004; 23(10):1292-300.
19. O'Duda R, Peter EH, David GS. Pattern classification. 2nd edition. John Wiley and Sons, 2001.
20. Hill CR, Bamber JC, ter Haar GR. Physical Principles of Medical Ultrasonics. John Wiley and Sons, 2004.
21. George DL. The velocity of sound through tissues and the acoustic impedance of tissues. J Acoust Soc Am 1950; 862-6.
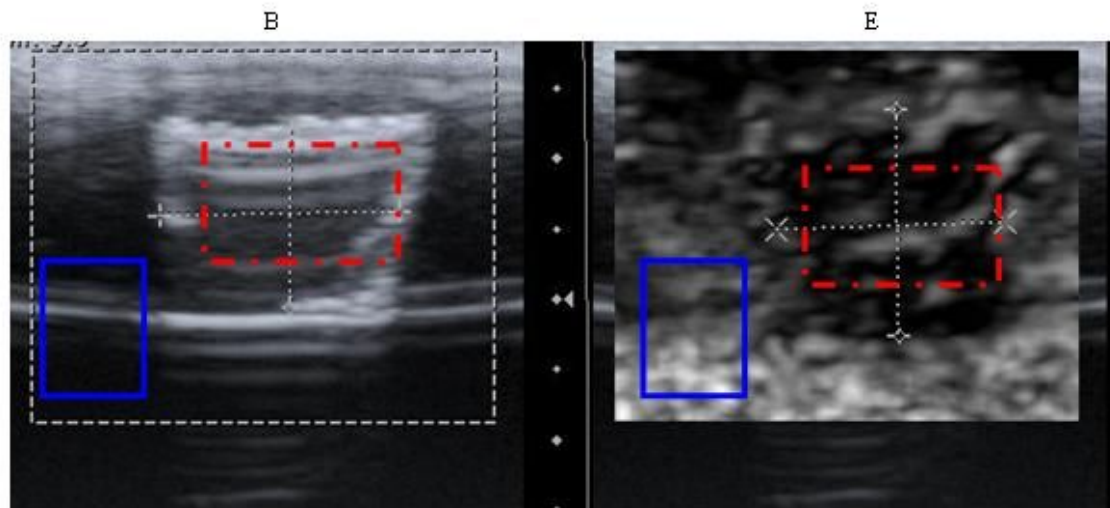
K Kumar et al. Biomed Imaging Interv J 2009; 5(4):e30

6
This page number is not
for citation purposes

Figure 6 Ultrasound B mode image (B) and elastogram (E) of a hyperechoic lesion. Rectangular region marked in red (dashed line) in B represents the lesion in B mode image selected for parameter measurement and region marked in blue (solid line) is the region in surroundings selected for parameter measurement. Rectangular region marked in red (dashed line) in E represents the lesion in elastogram selected for average strain measurement and region marked in blue (solid line) is the region in surroundings selected for average strain measurement.

Table 1 Acoustic parameters of the designed phantom with corresponding parameters for human tissue [20], [21] for comparison.

Parameters	Human Tissue	Values Obtained
Velocity (m/s)	1490 – 1610 (mean value: 1540)	1529.90
Attenuation (db/MHz-cm)	0.4 – 2.0 (mean value: 0.7)	0.66
Acoustic Impedance $\times 10^{-6}$ (kg/m^2-s)	1.58 – 1.70 (mean value: 1.63)	1.60

Table 2 Performance of selected parameters

Parameter	M	SK	ENT	ASM	max_prob	STR
AROC	0.59	0.51	0.56	0.58	0.52	0.73

Table 3 Classification accuracy with and without strain parameter

Parameters considered	Classification accuracy
Without STR	66.7% (10/15)
With STR	86.6% (13/15)